

Integration of Pixy2 Camera Sensor and Coordinate Transformation for Automatic Color-Based Implementation of a Pick-and-Place Arm Robot

Erwin Sitompul¹, Muhammad Teguh Ilham Yaqin¹, Hendra Jaya Tarigan², George Michael Tampubolon³,
Faisal Samsuri⁴, Mia Galina¹

¹President University, Jababeka Education Park, Cikarang, Indonesia

²Department of Engineering, Computer Science and Physics, School of Science and Mathematics,
Mississippi College, Mississippi, USA

³School of Mechanical Engineering, Pusan National University, Busan, South Korea

⁴Institute of Automation and Control, National Taiwan University of Science and Technology, Taiwan

ARTICLE INFO

Article history:

Received February 17, 2025

Revised March 06, 2025

Accepted March 20, 2025

Keywords:

Arm Robot;
Pick-and-Place;
Object Position Detection;
Object Color Recognition;
Coordinate Transformation

ABSTRACT

Technology related to robotics has developed rapidly in recent years. In manufacturing production lines, an industrial pick-and-place robot is used to efficiently move objects from one location to another. In most approaches, this robot automates the repetitive task from one exact start position. However, the task of collecting objects from various positions in the robot workspace still introduces challenges in terms of object positional detection and movement accuracy. In this paper, an arm robot system equipped with automatic color-based object recognition and position control was proposed. The robot was able to detect multiple target object positions automatically without any need to plan a fixed movement beforehand. In the construction of the experiment platform, a Pixy2 camera sensor with color recognition ability was integrated into a 4-DoF Dobot Magician arm robot. Furthermore, a coordinate transformation was derived and implemented to achieve an accurate positional robot movement. The coordinate transformation performed a mapping from the Camera Coordinate System (CCS), which was initialized from image pixel values to the Robot Coordinate System (RCS), which was finalized to the robot's actuator input signals. Prior to the implementation, the robot underwent a color calibration and position calibration. Thereafter, a set of color signatures was obtained and any object position in the camera's field of view can be matched with any end-effector position in the robot's workspace. Three experiment setups were conducted to evaluate the proposed system. Limited to one lighting condition, the robot was commanded to pick-and-place objects based on the criteria of all 3 colors, 1 specific color, and 2 specific colors. The robot performed perfectly to pick and place the objects, achieving a 100% success rate in terms of object color detection and pick-and-place. The positive results encouraged further investigation in different actuator actions and greater work areas.

This work is licensed under a [Creative Commons Attribution-Share Alike 4.0](https://creativecommons.org/licenses/by-sa/4.0/)



Corresponding Author:

Erwin Sitompul, President University, Jababeka Education Park, Cikarang 17550, Indonesia

Email: sitompul@president.ac.id

1. INTRODUCTION

Technology related to robotics has developed rapidly in the past years. This enables the robots to take more parts in helping humans complete tasks or jobs that go beyond the physical and safety limits of humans [1], [2], [3]. The innovation in robot application also synergizes with the trending advances in artificial intelligence, as can be found in the implementation of robots to support automation in agricultural activities

[4], [5], [6]. Furthermore, through the use of robots, production consistency and efficiency in various industrial sectors can be increased, by the contributions in conducting automatic extended-time defect detection, scheduled service, and repetitive tasks [7], [8],[9], [10]. Proper design and deployment of robot manipulators in the manufacturing industry have also improved the work process effectiveness and product quality [11], [12]. In this case, the manipulators had been made multifunctional and carried out various tasks in moving objects through programmed movements [13], [14], [15]. One robot task generally found in a manufacturing production line is moving material or products from one place to another or a pick-and-place task. In this particular application, the accuracy in positioning the robot's end-effectors after detecting the object's exact location is required. An inverse kinematics approach in modeling an arm robot for a pick-and-place task was reported in [16]. Besides, robots with pick-and-place tasks were proven to be implementable in processes that require fast response and high power to cope with heavy loads [17], [18]. To locate the points in the work area accurately, pick-and-place robots from recent developments utilized a camera as the vision sensor [19]. In addition, a robot equipped with a camera also requires an accurate mapping between a position in the camera's field of view and a corresponding position in the robot's space of movement [20], [21], [22]. The growing application of artificial intelligence and computer vision contributed to the multiplied number of research in this area with various robot application fields [23], [24], [25]. By having the ability to pinpoint the desired location directly from the camera, complex mathematical modeling such as in [26], [27] can be avoided, provided that the necessary actuator inputs to the robot can be determined accurately.

This study presented the integration of a camera sensor and coordinate transformation into a pick-and-place arm robot. This enabled the robot to identify the target object's position and color accurately and move the object from any position in the robot work area to a predefined collection area. The experiment platform was built around a Dobot Magician Robot and a Pixy2 camera sensor. A forward kinematic analysis of the Dobot Magician robot was conducted in [28], with an accuracy that reflects the real robot's ability to perform fine motor movements such as writing [29]. In its original condition, the robot was able to perform three-dimensional movements through manual inputs given from a control pad. The robot could also be commanded to move according to a sequence of recorded positions. This sensorless operation limited the functionality of the robot as it could not pick objects from an arbitrary position [30]. The built-in ability of the Pixy2 sensor camera in color-based object recognition was utilized and tuned to locate the coordinates of the target object correctly. Subsequently, a coordinate transformation mechanism was carefully derived and implemented, to enable accurate movement of the robot and its end-effector. To simplify the calculation process, the proposed coordinate transportation assumed a linear connection among the calibration points, and the rotation angle was represented by the horizontal axis rotation [31], [32]. The research contribution is to obtain a robot with an upgraded condition, where the robot could directly detect specific target objects' positions and move them consecutively. The experiments involved bottle caps in four different colors as the target objects. Three experiment setups were undertaken to prove the accuracy of the proposed system in terms of object color detection and object pick-and-place movement.

2. METHODS

2.1. Dobot Magician Robot and Pixy2 Camera Sensor

In practice, arm robots are among the most popular robot types used to support a production line [33][34]. An arm robot consists of a series of links connected by joints. The degree of movement, the shape of the workspace, and the potential applications of an arm robot are determined by the type and the number of its joints, which may vary based on the robot's design [35]. The joints allow the robot links to move in various directions, including translational and rotational movements [36], [37]. Later on, the end-effector, a device attached to the end of a robot link to help it interact with the surrounding environment, is chosen based on the required application, such as gripping, cutting, spraying, sanding, or welding.

The experiment platform in this research was built by utilizing a Dobot Magician Robot, as shown in Fig. 1. This robot has four degrees of freedom and high precision due to the use of four-bar links to drive the rotation of each link. Additionally, this robot uses a parallelogram mechanism to ensure that the orientation of the end-effector remains constant. Besides, this robot can be connected to various types of sensor modules and end-effectors. In its standard operation, the robot works without any sensor. The movements are based on recording and playing back a sequence of positions and actions.

However, the Dobot Magician robot can be made to work automatically through a microcontroller with an appropriate embedded program. In this research, the proposed control system consists of an Arduino Mega microcontroller, a Pixy2 camera sensor, and a vacuum suction cup end-effector as the actuator. Both the sensor and the actuator are shown in Fig. 2. The camera sensor is utilized to locate the position of a target object in a work area while also identifying the object's color. Through this control system, the robot can be calibrated to

automatically move the end-effector to any accurate coordinate in the work area to pick and place a target object based on color.



Fig. 1. Dobot Magician robot

The Pixy2 camera sensor is able to identify objects based on color through its built-in function. The camera matched various needs for vision not only in robotics applications [38], [39], [40]. camera has 256 kB RAM and 2 MB memory. The highest image resolution available is 1296×976 captured at a rate of 60 frames per second. The camera cannot identify objects based on shapes. Thus, the camera functions the best in an application where the objects involved are uniform in shape and each object has a single color [41], [42]. After the color data is recorded with the consideration of hue and brightness, the camera will locate any section on its field of view that matches the recorded colors.

In the following sections, the Dobot Magician robot will be referred to as the robot and the Pixy2 camera sensor will be referred to as the camera. By implementing a camera, the robot can perform movements beyond predetermined paths [43], [44].

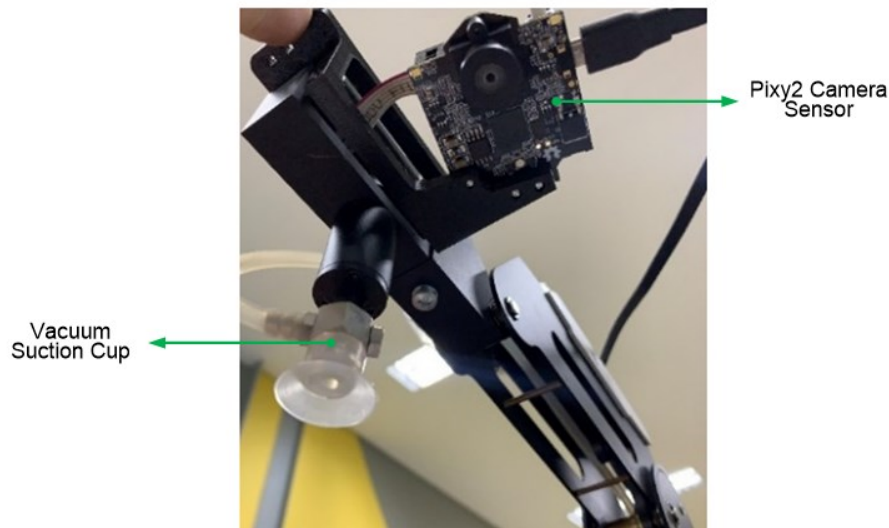


Fig. 2. The Pixy2 camera sensor and the vacuum suction cup

2.2. Coordinate Transformation

Both the robot and the camera have their own coordinate system. The robot coordinate is based on the input values given to its stepper motors, while the coordinate of the image captured by the camera is based on the pixel values. In order for the robot to be able to move accurately to a certain position, the camera coordinate system must be matched with the robot coordinate system. Once both coordinates are matched, the robot can be commanded to reach a certain position based on the camera capture. The matching process starts with the conversion of a desired position on the image taken by the camera to the Camera Coordinate System (CCS). These CCS values are then transformed into the Robot Coordinate System (RCS). Subsequently, each stepper motor of the robot's 4 axes can be given the necessary inputs to move the end-effector to a desired position.

The illustration of coordinate transformation is given in Fig. 3. The domain of the transformation is the CCS, while the range of the transformation is the RCS. The calibration points of the CCS are A_1 , B_1 , and C_1 , while those of the RCS are A_2 , B_2 , and C_2 . The calibration points in a coordinate system are chosen to be the point of origin, the rightmost point on the horizontal axis, and the topmost point on the vertical axis. For the sake of simplification, the rotation angle is calculated from the horizontal axis only and the curved image caused by lens distortion was neglected.

Forward kinematics analysis occurs when the translation of CCS coordinates A_1 , B_1 , and C_1 is converted into RCS coordinates A_2 , B_2 , and C_2 . In its original concept [45], [46], forward kinematics does not necessitate automation because the position of each axis is determined without considering the position of the end effector. This is different from inverse kinematics, where the position of the end effector is determined first, and the control system then performs a backward calculation using the end effector's position as a reference. However, the input from CCS A_1 , B_1 , and C_1 does not directly determine the final position of the end effector. Instead, it is interpreted as an instruction to move the axes by translating the position to RCS A_2 , B_2 , and C_2 , enabling automation, and allowing the end effector to move to the desired position according to feedback from the camera.

As also can be seen from Fig. 3, the points of origin A_1 given from the camera capture and A_2 given from the robot calibration may not give zero values and may create an angle with the respective true horizontal x -axis. However, shifting constants τ_1 and τ_2 can be determined to translate between A_1 to O_1 and A_2 to O_2 , and vice versa, respectively. Then, the shifting constants are to be applied to any points in the respective coordinate system to neutralize the effect of a non-zero point of origin. Afterward, the inclination angles θ_1 between the x' -axis and the x -axis in the CCS and the inclination angle θ_2 between the x'' -axis and the x -axis in the RCS can be used to rotate the coordinates accordingly, in order to neutralize the effect of the inclination angles.

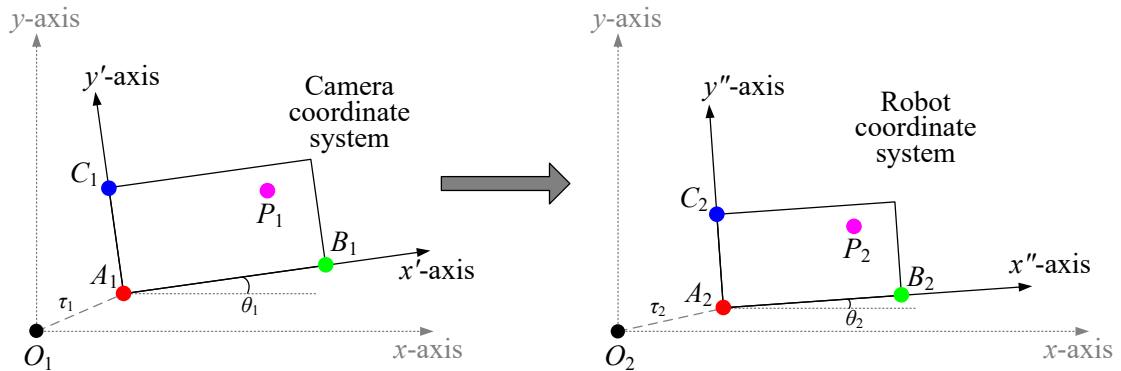


Fig. 3. The transformation from the initial coordinate to the final coordinate

In order to locate the end-effector of the robot to a target point captured by the camera at P_1 in the CCS, a corresponding point P_2 in the RCS must be first determined. This mapping from P_1 to P_2 is performed through the coordinate transformation. First, the point P_1 is to be translated by a subtraction with τ_1 to remove the non-zero origin. Then, the resulting coordinate is rotated by θ_1 clockwise to remove the effect of the inclination angle. Afterward, P_2 is calculated using the vertical and horizontal scaling between the CCS and the RCS. Subsequently, P_2 is rotated by θ_2 in a counterclockwise direction to reinstate the inclination angle and translated by adding τ_2 to restore the non-zero origin.

The steps of the coordinate transformation from the CCS to the RCS are summarized in Fig. 4. Fig. 5 shows the rotation at the CCS from $P_1(x'_1, y'_1)$ to become $P_1(x_1, y_1)$ as an example. The shifting constants are the coordinates A_1 and A_2 , $\tau_1 = (a_{1x}, a_{1y})$ and $\tau_2 = (a_{2x}, a_{2y})$, respectively, so that the translated coordinate of the points can be given by the equations:

$$x'_1 = x'_i - a_{1x}, y'_1 = y'_i - a_{1y} \quad (1)$$

$$x''_f = x''_2 + a_{2x}, y''_f = y''_2 + a_{2y} \quad (2)$$

The rotation angles are determined by the following equations:

$$\theta_1 = \cos^{-1} \left(\frac{b_{1x} - a_{1x}}{r_1} \right) \quad (3)$$

$$\theta_2 = \cos^{-1} \left(\frac{b_{2x} - a_{2x}}{r_2} \right) \quad (4)$$

where

$$r_1 = \sqrt{(b_{1x} - a_{1x})^2 + (b_{1y} - a_{1y})^2} \quad (5)$$

$$r_2 = \sqrt{(b_{2x} - a_{2x})^2 + (b_{2y} - a_{2y})^2} \quad (6)$$

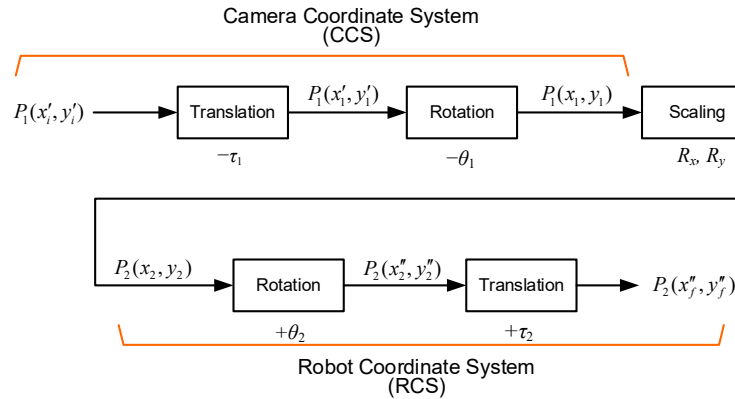


Fig. 4. The summary of coordinate transformation

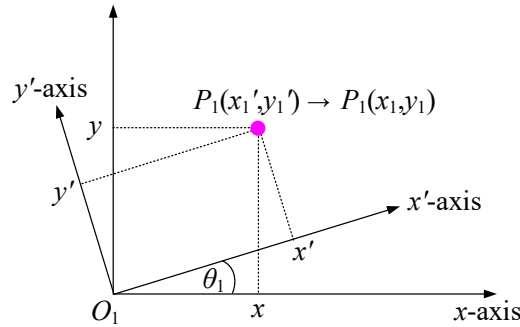


Fig. 5. The axis rotation to match the x' -axis with the x -axis.

It can be derived that $P_1(x'_1, y'_1)$ can be rotated to $P_1(x_1, y_1)$ using the following equations:

$$x_1 = x'_1 \cos \theta_1 - y'_1 \sin \theta_1 \quad (7)$$

$$y_1 = x'_1 \sin \theta_1 + y'_1 \cos \theta_1 \quad (8)$$

The rotation from $P_2(x_2, y_2)$ to $P_2(x''_2, y''_2)$ at the RCS can also be derived to be:

$$x_2'' = x_2 \cos \theta_2 + y_2 \sin \theta_2 \quad (9)$$

$$y_2'' = -x_2 \sin \theta_2 + y_2 \cos \theta_2 \quad (10)$$

Furthermore, the horizontal and vertical scaling ratios from $P_1(x_1, y_1)$ of the initial coordinate system (CCS) to the $P_2(x_2, y_2)$ of the final coordinate system (RCS) are given by R_x and R_y , respectively.

$$R_x = \frac{A_2 B_2}{A_1 B_1} = \frac{\sqrt{(b_{2x} - a_{2x})^2 + (b_{2y} - a_{2y})^2}}{\sqrt{(b_{1x} - a_{1x})^2 + (b_{1y} - a_{1y})^2}} \quad (11)$$

$$R_y = \frac{A_2 C_2}{A_1 C_1} = \frac{\sqrt{(c_{2x} - a_{2x})^2 + (c_{2y} - a_{2y})^2}}{\sqrt{(c_{1x} - a_{1x})^2 + (c_{1y} - a_{1y})^2}} \quad (12)$$

The formulas that govern the scaling process are given by:

$$x_2 = R_x x_1 \quad (13)$$

$$y_2 = R_y y_1 \quad (14)$$

Summarizing the coordinate transformation, the process will transform the position of any target object at its initial point $P_1(x_i, y_i)$ of the CCS to its final point $P_2(x_f, y_f)$ of the RCS. By feeding the robot with the value of the final point P_2 , the robot will be able to accurately move the end-effector to P_2 as the expected position to perform the planned action of pick-and-place.

2.3. Block Diagrams and Hardware Wiring

The block diagram of the proposed system is presented in Fig. 6. The red arrows represent the high-current power flow, while the blue arrows show the low-current power flow or the information flow. The Arduino Mega microcontroller is connected to the robot's stepper motors and the air pump through a UART (universal asynchronous receiver-transmitter) interface. The air pump supplies the required pressure for the vacuum suction cup to function. The microcontroller is also connected to an LCD keypad shield as input and output interface for the system. The keypad can be used to manually control the robot to reach a certain position. This is required during the position calibration of the robot. The motor settings to reach the calibration points are recorded in the microcontroller EEPROM memory and can be seen on the LCD.

The camera sensor is connected to the Arduino via the ICSP connector. At the same time, the covered area of the camera can also be observed in real time through the Pixy2Mon software installed on a laptop. For this purpose, the laptop is to be connected to the camera using a USB cable. An AC power source directly supplies the air pump and the motors.

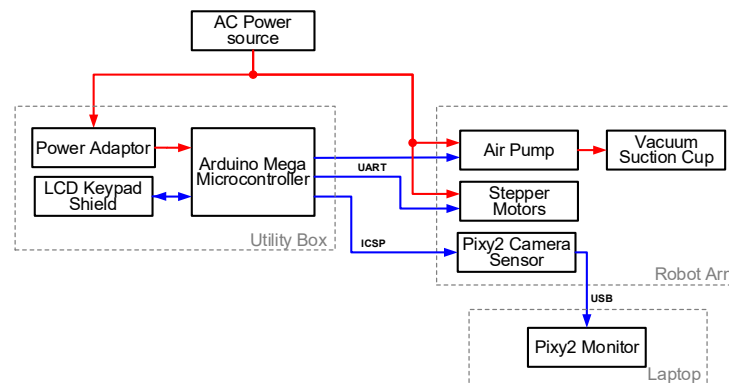


Fig. 6. The block diagram of the proposed system

When the camera detects a target object with a certain color in the work area, the object's coordinate in the two-dimensional plane will be sent to the microcontroller via the serial communication line. Afterward, the data is processed and the resulting output triggers the motors to move the robot links and the end-effector to the location of the object. At the end of this stage, the suction cup is already in a pressed position toward the object. Then, the microcontroller will send a signal to turn on the air pump to create an air vacuum which will enable the suction cup to stick on the object. Subsequently, the robot can pick the object and place it in a collection container. This process is repeated until the camera does not detect any object that fulfills the color criteria.

The pin connections between the microcontroller, the camera, the LCD keypad, and the UART terminal are shown in Fig. 7. The serial connection between the microcontroller and the robot through the UART terminal requires the connection of the pins TX, RX, and GND of the microcontroller.

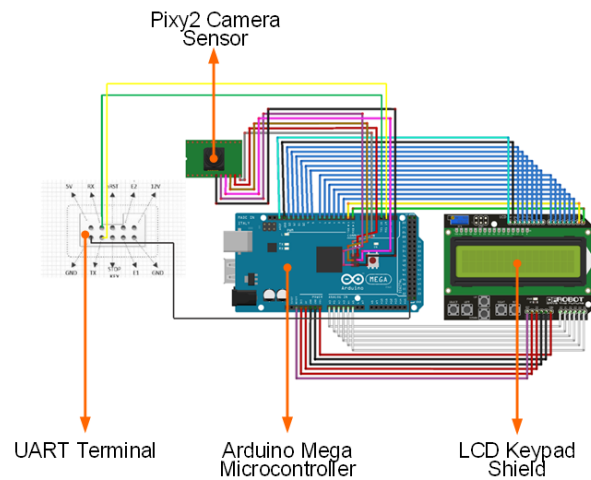
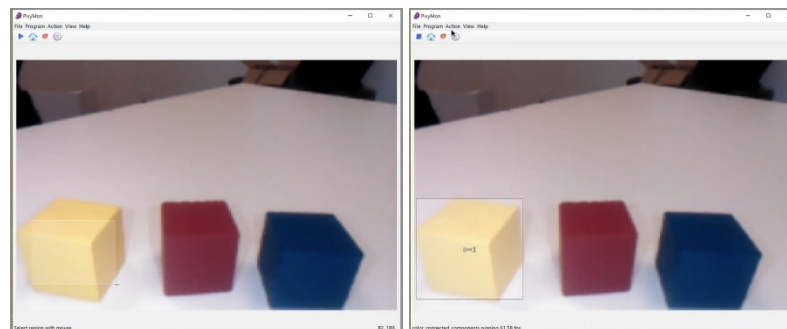


Fig. 7. The pin connections

2.4. Calibration Procedure and System Flowchart

The calibration phase of the proposed system consists of the *camera color calibration* and the *robot position calibration*. During the color calibration, the camera is operated to detect the colors of the target objects that will be picked and placed. The camera identifies the objects based on color and not shape. The camera can be set for hue and brightness to achieve the best calibration result. Furthermore, it is crucial to have the same lighting condition between the calibration phase and the operation phase.

The process of obtaining the color signature, which is the RGB color values of a target object, is shown in Fig. 8. The yellow cube as the target object is put in front of the camera and its area is manually selected, as shown in Fig. 8(a). After the signature is saved, the camera will put the label “s=1” any time it detects the object, as can be seen in Fig. 8(b). As can be seen, the color recognition algorithm can extrapolate the color range beyond the selected region. This results in a larger detection area compared to the selection area. Up to seven colors can be saved in the database, *i.e.*, in this experiment red, green, blue, and orange. All color signatures are then recorded in the EEPROM of the microcontroller for further use during the operation phase.



(a) (b)
Fig. 8. The addition of a color signature;
(a) Color selection area, (b) Color detection area

In the robot position calibration, the input settings of the robot motors to reach the boundaries of the work area are determined. This process requires a calibration card as seen in Fig. 9. The calibration card is to be put precisely on the desired work area and within the camera’s field of view [47], [48]. Then, the robot is given manual input via the keypad so that the end-effector can reach the 3 calibration points, which are the point of origin A , the rightmost point of the horizontal axis Bc and the topmost point of the vertical axis C . Furthermore, the default position and the home position of the robot. The default position is the position of the robot in a rest position between two operations, while the home position is the one where it will start and finish a pick-and-place cycle. Finally, the collection point where the robot will release and place the object in a collection container is to be determined. The scope of the robot was given fixed in the form of a working area. Further limitations excluded the consideration of overlapping objects, partial occlusions, and workspace dynamic changes.

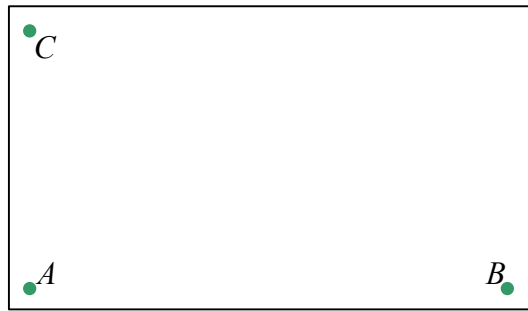


Fig. 9. The card used in the work area calibration

The flowchart of the proposed system during the operation phase is shown in Fig. 10. At the start, the camera and the robot need to be turned on and initialized. The functionality of the camera can also be checked first through the PixyMon software on the laptop. Afterward, the start button needs to be selected via the keypad and the robot will move from the default position to the home position. From this moment, the camera will scan the work area continuously and detect the presence of any target objects that fulfill the recorded color signatures. Then, the coordinate of the target objects in the CCS is sent one by one to the microcontroller and the coordinate transformation calculation will be conducted to determine the corresponding values in the RCS. The target object coordinates in the RCS are then sent to the robot’s actuators, the stepper motors so that the robot end-effector can move to the target object position.

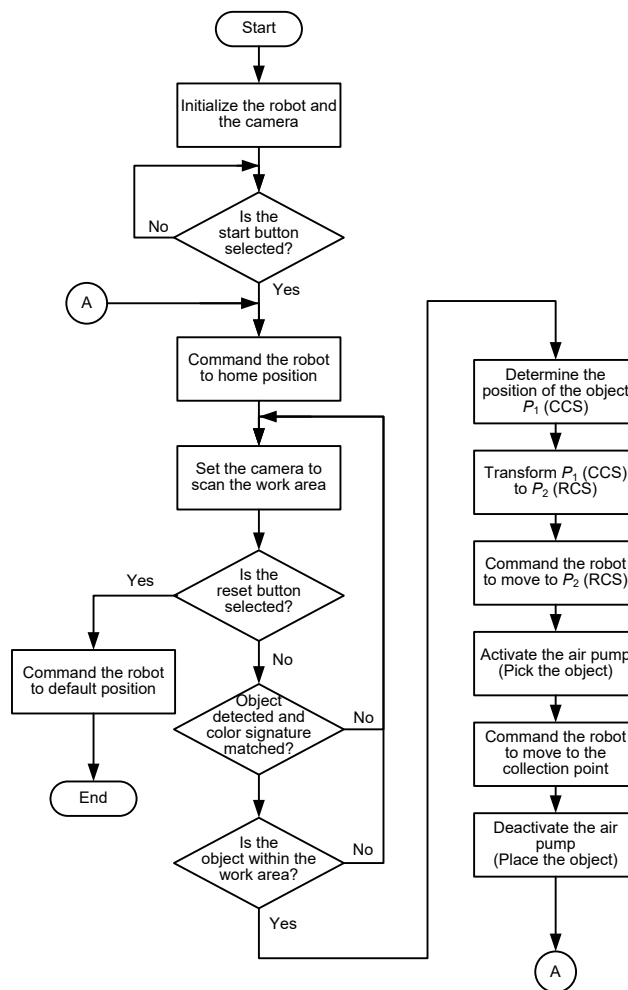


Fig. 10. The flowchart of the operation phase

After reaching the target object position, another actuator, the air pump will be activated so that the end effector, the vacuum suction cup, can pick the object. Afterward, the robot starts to move the object to the collection container and upon reaching it, releases the object into the collection container when the air pump is deactivated by the microcontroller. At this point, if the reset button is selected, the whole operation will be terminated and the robot goes to its default position. Otherwise, the robot will move to its home position to detect the next potential target object. Thus, the proposed robot operated in a feedforward scheme, where the correlation between the camera sensor and the robot's actuators is conducted once before the application phase [49], [50].

3. RESULTS AND DISCUSSION

3.1. Experiment Platform and System Calibration

The realization of the overall experiment platform of the proposed system can be seen in Fig. 11. During the operation, the use of a laptop is optional. The PixyMon software run on a laptop can be used to observe the area captured by the camera. The screenshot of the PixyMon can be seen in Fig. 12. As can be seen in Fig. 11 and Fig. 12, the target objects used are bottle caps with a diameter of 3.25 cm. The target objects exist in 3 different colors red, green, and blue. Additional yellow bottle caps are also used as a distraction.

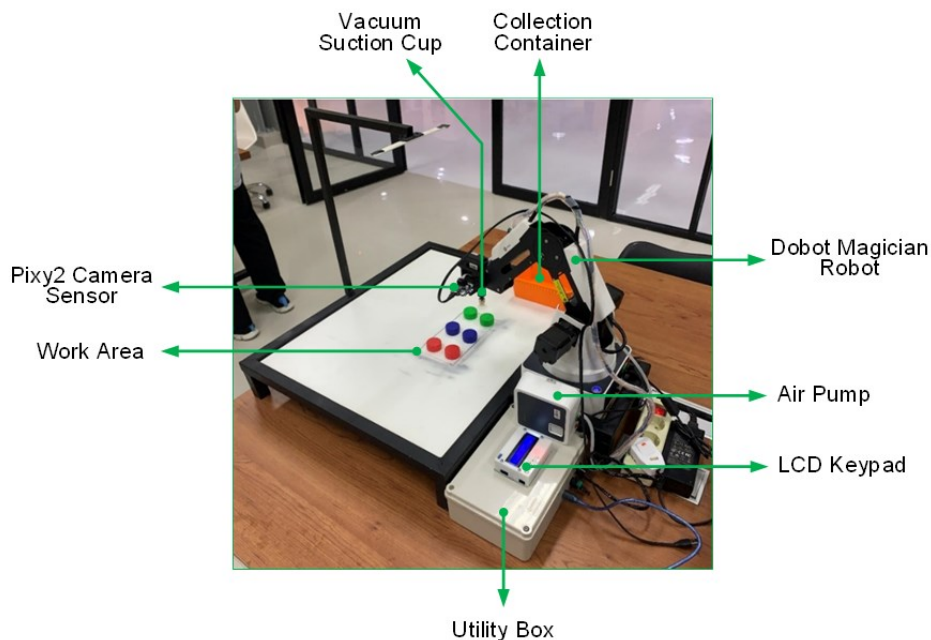


Fig. 11. The overall experiment platform of the pick-and-place arm robot system



Fig. 12. The PixyMon displays the work area as captured by the camera

3.2. Experiment Setup

After the completion of the calibration phase, the proposed system entered the operation phase, where it was tested for functionality and success rate. These were evaluated through a total of three experiment setups and 21 trials. A certain task was given to the robot, whether to pick and place target objects with one, two, or

three specific colors. In each trial, two bottle caps from each color red, green, and blue were placed within the work area as the target objects. Additional objects were also put outside the work area and served as distracting objects. Table 1 shows the summary of the experiment setups.

Table 1. Summary of the Experiment Setups

| Experiment Setup | Number of Target Colors | Target Colors | Number of Trials |
|------------------|-------------------------|---------------------------------|------------------|
| 1 | 3 | R, G, and B | 3 |
| 2 | 1 | R G B | 3 each |
| 3 | 2 | R and G, R and B, G and B | 3 each |

*R : Red, G : Green, B : Blue

Two success rates were used to assess the proposed system in terms of the color detection performance and the pick-and-place performance, as described in (15) and (16). The color detection success rate measures the ability of the camera to detect the colors correctly, while the pick-and-place success rate shows the ability of the robot's actuators to perform the task of picking and placing the target objects.

$$\text{Color detection success rate} = \frac{\text{Number of objects with correct color detection}}{\text{Total number of objects to detect}} \times 100\% \quad (15)$$

$$\text{Pick - and - place success rate} = \frac{\text{Number of objects with successful pick - and - place}}{\text{Total number of objects pick - and - place}} \times 100\% \quad (16)$$

3.3. Experiments

Experiment Setup 1

In Experiment Setup 1, all target objects in the work area were expected to be detected and moved successfully. The target colors in this setup were the colors Red (R), Green (G), and Blue (B), each with 2 caps. The setup was repeated in 3 trials. The results of the Experiment Setup 1 are summarized in Table 2. The Color Detection Success Rate and the Pick-and-Place Success Rate are presented in two separate columns.

The start point in one trial as viewed by the camera is depicted in Fig. 13. Here, six objects were identified as the targets, as can be seen by the boxes generated to mark the targets. As a representative, the chronological action of one trial is presented in Table 3. The image scanned by the PixyMon in Fig. 13 is rotated by 180° to ease the comparison between this image and the images in Table 3.

Table 2. Results of Experiment Setup 1

| Trial Number | Target Color and Quantity | Target Count | Color Detection Success Rate (%) | Pick-and-Place Success Rate (%) |
|--------------|---------------------------|--------------|----------------------------------|---------------------------------|
| 1 | 2 R, 2 G, 2 B | 6 | 100 | 100 |
| 2 | 2 R, 2 G, 2 B | 6 | 100 | 100 |
| 3 | 2 R, 2 G, 2 B | 6 | 100 | 100 |

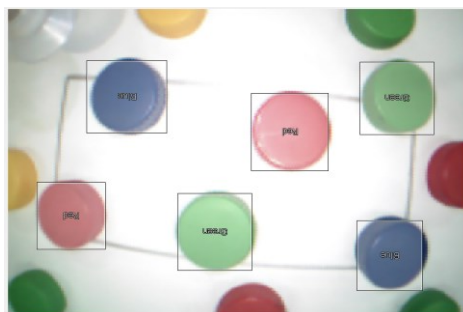

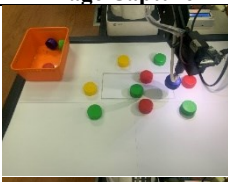

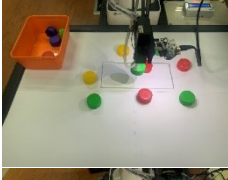
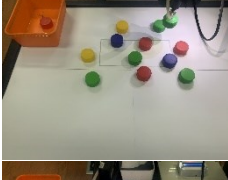


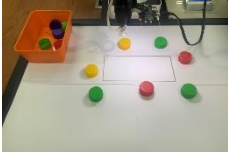


Fig. 13. The start of one trial in Experiment Setup 1 as detected by the camera (Target: Red, Green, and Blue)

Table 3. The Chronological Action in One Trial of Experiment Setup 1
(Target: Red, Green, and Blue)

| Sequence | Action | Image Capture | Sequence | Action | Image Capture |
|----------|-----------|--|----------|-----------|--|
| 1 | Start |  | 5 | Picking B |  |
| 2 | Picking R |  | 6 | Picking G |  |
| 3 | Picking G |  | 7 | Picking R |  |
| 4 | Picking B |  | 8 | Finish |  |

Experiment Setup 2

In Experiment Setup 2, one target color was set at a time and the ability of the proposed system to only move target objects with one specific color was tested. For each of the target colors Red, Green, and Blue, the setup was repeated in three trials. The results are summarized in Table 4.

As the first representative, the start point in one trial with Red as the target as viewed by the camera is depicted in Fig. 14. Here the red caps were boxed and identified as the target objects. The chronological action of one trial with Red as the target is presented in Table 5.

As the second representative, for the green caps as the target objects, the start point is shown in Fig. 15. Here the green caps were boxed and identified as the targets. The chronological action of one trial with Green as the target is presented in Table 6.

Table 4. Results of Experiment Setup 2

| Target Color and Quantity | Number of Trials | Target Count | Color Detection Success Rate (%) | Pick-and-Place Success Rate (%) |
|---------------------------|------------------|--------------|----------------------------------|---------------------------------|
| 2 R | 3 | 6 | 100 | 100 |
| 2 G | 3 | 6 | 100 | 100 |
| 2 B | 3 | 6 | 100 | 100 |

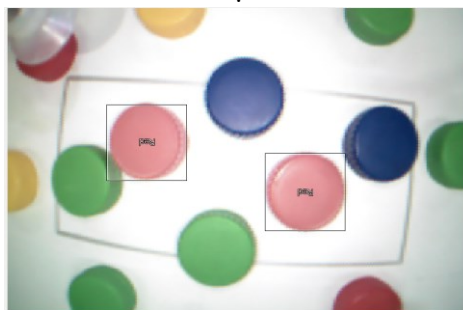

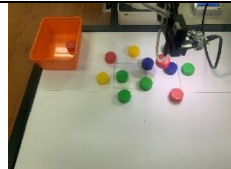
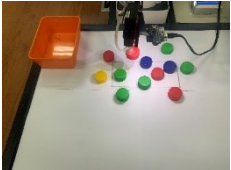



Fig. 14. The start of one trial in Experiment Setup 2 as detected by the camera (Target: Red)

Table 5. Chronological Action in One Trial of Experiment Setup 2
(Target: Red)

| Sequence | Action | Image Capture | Sequence | Action | Image Capture |
|----------|-----------|---|----------|-----------|---|
| 1 | Start |  | 3 | Picking R |  |
| 2 | Picking R |  | 4 | Finish |  |

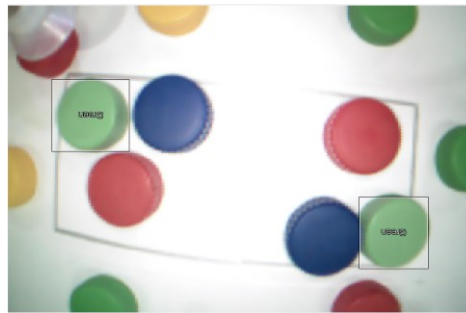
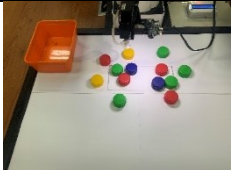
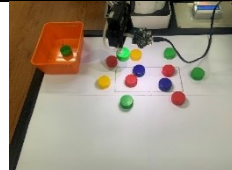

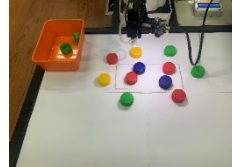


Fig. 15. The start of one trial in Experiment Setup 2 as detected by the camera (Target: Green)

Table 6. Chronological Action in One Trial of Experiment Setup 2
(Target: Green)

| Sequence | Action | Image Capture | Sequence | Action | Image Capture |
|----------|-----------|---|----------|-----------|---|
| 1 | Start |  | 3 | Picking G |  |
| 2 | Picking G |  | 4 | Finish |  |

Experiment Setup 3

In Experiment Setup 3, one color was excluded and not moved during the pick-and-place process. The other two colors were moved to the collection container. The results of the Experiment Setup 3 are presented in [Table 7](#).

Table 7. Results of Experiment Setup 3

| Target Color and Quantity | Number of Trials | Target Count | Color Detection Success Rate (%) | Pick-and-Place Success Rate (%) |
|---------------------------|------------------|--------------|----------------------------------|---------------------------------|
| 2 R and 2 G | 3 | 12 | 100 | 100 |
| 2 R and 2 B | 3 | 12 | 100 | 100 |
| 2 G and 2 B | 3 | 12 | 100 | 100 |

The first representative of the experiment results with the start point in one trial with Red and Green as the target as viewed by the camera is depicted in Fig. 16. Here the red and green caps were boxed and identified as the targets. The chronological action of one trial with Red as the target is presented in Table 8.

As the second representative, the same process was repeated with Red and Blue as the target. The corresponding observation and result are shown in Fig. 17 and Table 9.



Fig. 16. The start of one trial in Experiment Setup 3 as detected by the camera (Target: Red and Green)

Table 8. Chronological Action in One Trial of Experiment Setup 3 (Target: Red and Green)

| Sequence | Action | Image Capture | Sequence | Action | Image Capture |
|----------|-----------|---------------|----------|-----------|---------------|
| 1 | Start | | 4 | Picking G | |
| 2 | Picking R | | 5 | Picking R | |
| 3 | Picking G | | 6 | Finish | |

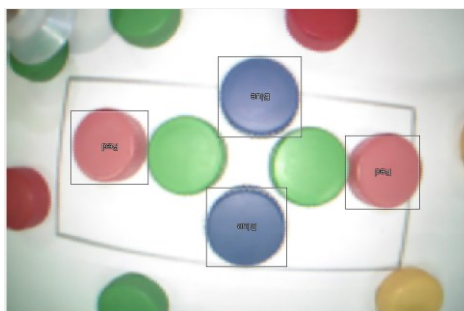

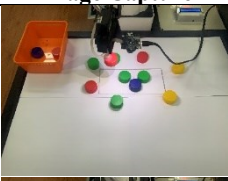

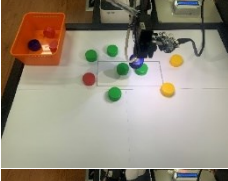

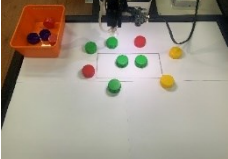


Fig. 17. The start of one trial in Experiment Setup 3 as detected by the camera (Target: Red and Blue)

Table 9. Chronological Action in One Trial of Experiment Setup 3
(Target: Red and Blue)

| Sequence | Action | Image Capture | Sequence | Action | Image Capture |
|----------|-----------|---|----------|-----------|---|
| 1 | Start |  | 4 | Picking R |  |
| 2 | Picking R |  | 5 | Picking B |  |
| 3 | Picking B |  | 6 | Finish |  |

3.4. Discussion

The proposed pick-and-place arm robot system with a Pixy2 camera sensor for object color detection and coordinate transformation for accurate object position detection was successfully integrated. After the color calibration phase and the position calibration phase, the robot was evaluated through three experiment setups to prove its ability to perform the pick-and-place task on target objects based on color. The target objects with the colors red, green, and blue, were to be moved from a work area to a collection container.

In Experiment Setup 1, a total of 18 target objects in all three colors were successfully identified, picked, and placed with a perfect 100% success rate in the category of color detection and the category of pick-and-place. Subsequently, in Experiment Setup 2, target objects with one color at a time were specified. Again, a total of 18 target objects were successfully detected and moved with a perfect 100% success rate in both categories. Finally, in Experiment Setup 3, the system was tested to detect target objects with two colors at a time, *i.e.*, red and green, red and blue, and green and blue. In total, there were 36 target objects involved and the system was able to identify the colors and move the objects with a 100% success rate in both categories.

The controlled conditions during the experiments were chosen to fully examine the contribution of object detection and coordinate transformation to improve the existing robot. Further variability regarding the environmental condition, target object shapes, and lighting depends on the feature offered by the camera that will be used. Separated artificial intelligence methods can be further developed to process the image obtained from the camera so that the robot can work in operate in a more general environment [51], [52], [53]. The positional calibration within the order of fractions of millimeter was proven adequate for the current robot operation such that no error propagation could be detected.

Besides the flawless operation of the vacuum suction cup as the actuator, the totally perfect success rate of 100% proved twofold. Firstly, the camera sensor has been correctly adjusted and the experiment condition could be equally maintained between the calibration phase and the operation phase. Secondly, the algorithm of the coordinate transformation used to map the Camera Coordinate System (CCS) to the Robot Coordinate System (RCS) has run accurately, enabling the robot's end-effector to reach the correct positions as detected by the camera.

The main challenge in preparing the system was encountered during the color calibration phase where the camera had to be adjusted a number of times for the best color signature range. For this purpose, the calibration procedure was repeated several times until the whole distinct color area of a target object could be identified and boxed by the camera's built-in algorithm. Furthermore, to ensure that the camera could scan the same target object with the same color hue and brightness, the illumination of the work area was maintained at the same condition during the color calibration phase and the operation phase. The vacuum suction cup was very influential to the pick-and-place performance of the system. The surface of the cup and those of the bottle caps used as the target objects had to be maintained in a clean condition to ensure that both surfaces could stick together strongly.

If required, the scalability of the proposed system to more complex environments or larger workspaces is excellent. The adjustment time and cost are low because any new implementation only requires the repetition of the calibration process, along with a supportive camera field of view and robot reachability.

4. CONCLUSION

The integration of a Pixy2 camera sensor and coordinate transformation to the control algorithm of a Dobot Magician arm robot was successfully conducted in this study. The integration of the camera along with an Arduino microcontroller into the existing arm robot created an automatic control system, with the objective to identify the target objects based on color, and subsequently perform an automatic pick-and-place, moving the target objects from any point within the work area to a collection container. The built-in object color recognition function of the camera enabled precise pinpoint of the object position and the derived coordinate transformation was required to map the object position as captured by the camera to the corresponding coordinate of the robot's work space. Three experiment setups were organized to test the overall system performance. In each trial, the robot was given the assignment to collect all target objects within the work area that fulfill specific color criteria. The robot performed perfectly in all trials of all setups and accomplished its objective, with a 100% success rate in terms of color detection and pick-and-place.

The results encourage further research involving arm robots in manufacturing-related tasks with other specific actuator actions and greater work areas. Besides, an online position calibration mechanism that includes inverse kinematics and a fixed-point camera can be further elaborated. In this case, the actuator inputs required by the end-effector to reach a certain position can be corrected during the operation, by comparing the position deviation as captured by the camera and calculating the required input adjustment based on the inverse kinematics equations. By doing this, the robot will be upgraded to a feedback control system and become less prone to robot actuator errors and to robot base positional changes.

ACKNOWLEDGMENTS

The authors would like to thank the Jababeka Fabrication Laboratory (FabLab), Cikarang, for the permission to use the arm robot along with the supporting equipment and tools required to perform this research.

REFERENCES

- [1] A. Alkamachi and Y. G. K. Abboosh, "Modelling and control of cable driven robotic arm using maplesim," *Advances in Electrical and Electronic Engineering*, vol. 22, no. 3, 2024, <https://doi.org/10.15598/aece.v22i3.5685>.
- [2] S. Li *et al.*, "An indoor autonomous inspection and firefighting robot based on SLAM and flame image recognition," *Fire*, vol. 6, no. 3, Feb. 2023, <https://doi.org/10.3390/fire6030093>.
- [3] Z. Wang, Y. Wu, and Q. Niu, "Multi-sensor fusion in automated driving: a survey," *IEEE Access*, vol. 8, pp. 2847–2868, 2020, <https://doi.org/10.1109/ACCESS.2019.2962554>.
- [4] S. M. Kesavan, K. S. Al Mamari, and N. S. M. Raja, "Solar powered robot for agricultural applications," in *2021 International Conference on System, Computation, Automation and Networking (ICSCAN)*, pp. 1-5, 2021, <https://doi.org/10.1109/ICSCAN53069.2021.9526436>.
- [5] E. Sitompul, M. R. Gubarda, P. Sihombing, T. Simarmata and A. Turnip, "Sprayer System on Autonomous Farming Drone Based on Decision Tree," in *2024 IEEE International Conference on Artificial Intelligence and Mechatronics Systems (AIMS)*, pp. 1-6, 2024, <https://doi.org/10.1109/AIMS61812.2024.10512852>.
- [6] H. Firdaus, R. Mardiaty, and A. E. Setiawan, "Tomato harvesting robot prototype: Fuzzy-controlled arm with vision-based tomato detection," in *2024 10th International Conference on Wireless and Telematics (ICWT)*, pp. 1–6, 2024, <https://doi.org/10.1109/ICWT62080.2024.10674688>.
- [7] E. Sitompul, V. L. Setiawan, H. J. Tarigan, and M. Galina, "Image classification of fabric defects using ResNet50 deep transfer learning in FastAI," *Bulletin of Electrical Engineering and Informatics*, vol. 13, no. 5, pp. 3255–3267, 2024, <https://doi.org/10.11591/eei.v13i5.8218>.
- [8] J. Holland *et al.*, "Service robots in the healthcare sector," *Robotics*, vol. 10, no. 1, p. 47, 2021, <https://doi.org/10.3390/robotics10010047>.
- [9] A. Perzylo *et al.*, "SMERobotics: Smart Robots for Flexible Manufacturing," *IEEE Robotics & Automation Magazine*, vol. 26, no. 1, pp. 78–90, 2019, <https://doi.org/10.1109/mra.2018.2879747>.
- [10] X. Han, P. Liu, and J. Zhang, "A small payload desktop industry robot design without conventional reducers," *International Journal of Robotics and Automation (IJRA)*, vol. 13, no. 1, p. 31, 2024, <https://doi.org/10.11591/ijra.v13i1.pp31-40>.
- [11] M.-L. Tseng, T. P. T. Tran, H. M. Ha, T.-D. Bui, and M. K. Lim, "Sustainable industrial and operation engineering trends and challenges Toward Industry 4.0: a data driven analysis," *Journal of Industrial and Production Engineering*, vol. 38, no. 8, pp. 581–598, Nov. 2021, <https://doi.org/10.1080/21681015.2021.1950227>.

- [12] C. Patruno, V. Renò, M. Nitti, N. Mosca, M. di Summa, and E. Stella, "Vision-based omnidirectional indoor robots for autonomous navigation and localization in manufacturing industry," *Heliyon*, vol. 10, no. 4, p. e26042, 2024, <https://doi.org/10.1016/j.heliyon.2024.e26042>.
- [13] A. M. Romanov, N. Gyrichidi, and M. P. Romanov, "A novel gripper with integrated rotary unit and force control for Pick and Place applications," *Robotics*, vol. 11, no. 6, p. 155, 2022, <https://doi.org/10.3390/robotics11060155>.
- [14] K. Komoda, S. Tokura, H. Eto, and A. Ogawa, "Grasping strategy to improve the grasping success rate for picking robots with suction and pinching mechanism," in *Proc. JSME Annu. Conf. Robot. Mechatron. (RoboMec)*, vol. 2021, no. 0, pp. 2A1-A06, 2021, <https://doi.org/10.1299/jsmermd.2021.2a1-a06>.
- [15] F. Fahmizal *et al.*, "Path planning for mobile robots on dynamic environmental obstacles using PSO optimization," *Jurnal Ilmiah Teknik Elektro Komputer dan Informatika (JITEKI)*, vol. 10, no. 1, pp. 166–172, 2024, <https://doi.org/10.26555/jiteki.v10i1.28513>.
- [16] A. R. Al Tahtawi, M. Agni, and T. D. Hendrawati, "Small-scale robot arm design with pick and place mission based on inverse kinematics," *Journal of Robotics and Control (JRC)*, vol. 2, no. 6, 2021, <https://doi.org/10.18196/jrc.26124>.
- [17] S. D. Han, S. W. Feng, and J. Yu, "Toward fast and optimal robotic pick-and-place on a moving conveyor," *IEEE Robotics and Automation Letters*, vol. 5, no. 2, pp. 446–453, 2020, <https://doi.org/10.1109/lra.2019.2961605>.
- [18] T. Anzai, M. Zhao, T. Nishio, F. Shi, K. Okada, and M. Inaba, "Fully autonomous brick pick and place in fields by articulated aerial robot: Results in various outdoor environments," *IEEE Robot. Autom. Mag.*, vol. 31, no. 2, pp. 39–53, 2024, <https://doi.org/10.1109/mra.2023.3276265>.
- [19] J. Hu, Y. Niu, and Z. Wang, "Obstacle avoidance methods for rotor UAVs using RealSense camera," in *2017 Chinese Automation Congress (CAC)*, pp. 7151–7155, Oct. 2017, <https://doi.org/10.1109/CAC.2017.8244068>.
- [20] T. Ishiguro, H. Okuda, and T. Suzuki, "Proposal of model predictive trajectory planning method for autonomous parking considering obstacle avoidance constraint with coordinate transformation," in *Proc. JSME Annu. Conf. Robot. Mechatron. (RoboMec)*, vol. 2021, no. 0, pp. 1A1-E07, 2021, <https://doi.org/10.1299/jsmermd.2021.1a1-e07>.
- [21] G. Soleti, P. R. Massenio, J. Kunze, and G. Rizzello, "Nonlinear coordinate transformation and trajectory tracking control of an underactuated soft robot driven by dielectric elastomers," in *2024 IEEE 7th International Conference on Soft Robotics (RoboSoft)*, pp. 228–234, 2024, <https://doi.org/10.1109/RoboSoft60065.2024.10521952>.
- [22] C. Tian, N. Hao, F. He, and H. Yao, "Consistent distributed cooperative localization: A coordinate transformation approach," in *IEEE/RSJ International Conference on Intelligent Robots and Systems (IROS)*, pp. 10297–10303, 2024, <https://doi.org/10.1109/IROS58592.2024.10802078>.
- [23] S.-H. Wu and X.-S. Hong, "Integrating computer vision and natural language instruction for collaborative robot human-robot interaction," in *2020 International Automatic Control Conference (CACCS)*, pp. 1–5, Nov. 2020, <https://doi.org/10.1109/CACCS50047.2020.9289768>.
- [24] C. D. Vo, D. A. Dang, and P. H. Le, "Development of multi-robotic arm system for sorting system using computer vision," *Journal of Robotics and Control (JRC)*, vol. 3, no. 5, pp. 690–698, 2022, <https://doi.org/10.18196/jrc.v3i5.15661>.
- [25] M. N. S. Zainudin, S. B. A. Radzi, M. S. J. B. A. Razak, W. H. B. M. Saad, and M. H. B. A. Razak, "RGB-depth map formation from cili-padi plant imaging using stereo vision camera," *International Journal of Computer Vision and Robotics*, vol. 1, no. 1, p. 1, 2022, <https://doi.org/10.1504/ijcvr.2022.10049137>.
- [26] S. Qiu and M. R. Kermani, "Precision fingertip grasp: A human-inspired grasp planning and inverse kinematics approach for integrated arm–hand systems," *Robotics and Autonomous Systems*, vol. 162, p. 104348, Apr. 2023, <https://doi.org/10.1016/j.robot.2022.104348>.
- [27] O. Hock and J. Sedo, "Inverse kinematics using transposition method for robotic arm," in *2018 ELEKTRO*, pp. 1-5, 2018. <https://doi.org/10.1109/ELEKTRO.2018.8398366>.
- [28] J. D. Sanjuan De Caro, M. Rahman, and I. Rulik, "Forward kinematic analysis of Dobot using closed-loop method," *IAES International Journal of Robotics and Automation (IJRA)*, vol. 9, no. 3, p. 153, 2020, <https://doi.org/10.11591/ijra.v9i3.pp153-159>.
- [29] Z. Wang *et al.*, "A magnetic soft robot with multimodal sensing capability by multimaterial direct ink writing," *Additive Manufacturing*, vol. 61, p. 103320, Jan. 2023, <https://doi.org/10.1016/j.addma.2022.103320>.
- [30] S. Sukamta, A. Nugroho, S. Subiyanto, R. Reziyanto, M. F. Soambaton, and A. Ardiyanto, "Image-based position control for three-wheel Omni-directional robot," *Jurnal Ilmiah Teknik Elektro Komputer dan Informatika (JITEKI)*, vol. 10, no. 3, pp. 566–579, 2024, <https://doi.org/10.26555/jiteki.v10i3.29601>.
- [31] P. Raykov, N. Valchkova, and R. Zahariev, "Analytical coordinate transformation for manipulation when using robots to serve people with disabilities," in *2022 International Conference on Electrical, Computer and Energy Technologies (ICECET)*, pp. 1-6, 2022, <https://doi.org/10.1109/ICECET55527.2022.9872603>.
- [32] Q. Guifang, S. U. N. Dalin, S. Guangming, W. E. N. Xiulan, W. E. I. Zhong, and S. Aiguo, "A rapid coordinate transformation method for serial robot calibration system," *Chinese Journal of Mechanical Engineering*, vol. 56, no. 14, p. 1, 2020, <https://doi.org/10.3901/jme.2020.14.001>.
- [33] S. Mondal, N. F. Sharon, K. M. Tabassum, U. H. Muna and N. Alam, "Development of a Low-Cost Real Time Color Detection Capable Robotic Arm," in *26th International Conference on Computer and Information Technology (ICCIT)*, pp. 1-6, 2023, <https://doi.org/10.1109/ICCIT60459.2023.10441038>.
- [34] M. Alshihabi, M. Ozkahraman, and M. Y. Kayacan, "Enhancing the reliability of a robotic arm through lightweighting and vibration control with modal analysis and topology optimization," *Mechanics Based Design of Structures and Machines*, pp. 1–25, 2024, <https://doi.org/10.1080/15397734.2024.2400207>.

- [35] R. Siemasz, K. Tomczuk, and Z. Malecha, "3D printed robotic arm with elements of artificial intelligence," *Procedia Computer Science*, vol. 176, pp. 3741–3750, 2020, <https://doi.org/10.1016/j.procs.2020.09.013>.
- [36] H.-S. Kim and J.-B. Song, "Multi-DOF counterbalance mechanism for a service robot arm," *IEEE/ASME Transactions on Mechatronics*, vol. 19, no. 6, pp. 1756–1763, Dec. 2014, <https://doi.org/10.1109/tmech.2014.2308312>.
- [37] T. T. Tung, N. Van Tinh, D. T. Phuong Thao, and T. V. Minh, "Development of a prototype 6 degree of freedom robot arm," *Results in Engineering*, vol. 18, Jun. 2023, <https://doi.org/10.1016/j.rineng.2023.101049>.
- [38] B. R. M. Oldan *et al.*, "Development of automatic solar-powered microcontroller- based algae collector using Pixy2 cam in taal lake," in *2024 5th Technology Innovation Management and Engineering Science International Conference (TIMES-iCON)*, pp. 1–5, 2024, <https://doi.org/10.1109/TIMES-iCON61890.2024.10630733>.
- [39] F. Morariu, T. Morariu, and S.-G. Racz, "Mobile robot vision navigation strategy based on Pixy2 camera," *Material Today: Proceedings*, vol. 93, pp. 636–640, 2023, <https://doi.org/10.1016/j.matpr.2023.04.327>.
- [40] S. D. Perkasa, P. Megantoro, and H. A. Winarno, "Implementation of a camera sensor pixy 2 CMUcam5 to A two wheeled robot to follow colored object," *Journal of Robotics and Control (JRC)*, vol. 2, no. 6, 2021, <https://doi.org/10.18196/26128>.
- [41] M. Nihad Noaman, Z. Yousif Abdoon Al-Shibaany, and S. Al-Wais, "Omnidirectional robot indoor localisation using two pixy cameras and artificial colour code signature beacons," in *The 3rd International Conference on Computational Intelligence and Intelligent Systems*, pp. 110-118, 2020, <https://doi.org/10.1145/3440840.3440849>.
- [42] S. Saxena and S. G. Neogi, "A Framework for Insight Finder by Object Detection Mechanism," in *8th International Conference on Reliability, Infocom Technologies and Optimization (Trends and Future Directions) (ICRITO)*, pp. 417-420, 2020, <https://doi.org/10.1109/ICRITO48877.2020.9198009>.
- [43] T. D. Tran, X. Q. Ngo, V. T. Duong, H. Hung Nguyen, and T. T. Nguyen, "Predetermined path tracking of dedicated mobile robot using Pixy2 sensor: Application for fire extinguisher testing," in *International Conference on Electrical, Communication and Computer Engineering (ICECCE)*, pp. 1-6, 2023, <https://doi.org/10.1109/ICECCE61019.2023.10442319>.
- [44] S. F. M. Putri, R. Mardiaty, and A. E. Setiawan, "The prototype of arm robot for object mover using Arduino Mega 2560," in *8th International Conference on Wireless and Telematics (ICWT)*, pp. 1–6, 2022, <https://doi.org/10.1109/ICWT55831.2022.9935416>.
- [45] A. Mohammad and A. Hassan, "Forward and inverse kinematics of a 6-DOF robotic manipulator with a prismatic joint using MATLAB toolbox," *International Journal of Advanced Technology and Engineering Exploration*, vol. 11, pp. 2394-7454, 2024, <https://doi.org/10.19101/IJATEE.2024.111100210>.
- [46] D. Hroncová, E. Miková, E. Prada, R. Rákay, P. Ján Sinčák and T. Merva, "Forward and inverse robot model kinematics and trajectory planning," *20th International Conference on Mechatronics - Mechatronika (ME)*, pp. 1-9, 2022, <https://doi.org/10.1109/ME54704.2022.9983355>.
- [47] L. Roveda, P. Veerappan, M. Maccarini, G. Bucca, A. Ajoudani, and D. Piga, "A human-centric framework for robotic task learning and optimization," *Journal of Manufacturing Systems*, vol. 67, pp. 68–79, Apr. 2023, <https://doi.org/10.1016/j.jmsy.2023.01.003>.
- [48] J. Civera, L. Terissi, T. Pire, H. Gonzalez, and E. Santano, "An experimental evaluation of feature detectors and descriptors for visual SLAM," *International Journal of Computer Vision and Robotics*, vol. 1, no. 1, p. 1, 2022, <https://doi.org/10.1504/ijcvr.2022.10047492>.
- [49] F. Faizah, A. Triwiyatno and R. R. Isnanto, "Fuzzy Logic Implementation on Motion of Tennis Ball Picker Robot," in *IEEE International Conference on Communication, Networks and Satellite (COMNETSAT)*, pp. 57-63, 2021, <https://doi.org/10.1109/COMNETSAT53002.2021.9530815>.
- [50] E. Sitompul, R. M. Putra, H. Tarigan, A. Silitonga, and I. Bukhori, "Implementation of digital feedback control with change rate limiter in regulating water flow rate using Arduino," *Buletin Ilmiah Sarjana Teknik Elektro*, vol. 6, no. 1, pp. 72–82, 2024, <https://doi.org/10.12928/biste.v6i1.10234>.
- [51] M. S. Hylmi, Wiharto, and E. Suryani, "Detection of potato leaf disease using multi-class support vector machine based on texture, color, and shape features," in *International Conference on Electrical and Information Technology (IEIT)*, pp. 20-24, 2022, <https://doi.org/10.1109/IEIT56384.2022.9967866>.
- [52] J. Baeg and J. Park, "Oriented bounding box detection robust to vehicle shape on road under real-time constraints," in *IEEE 26th International Conference on Intelligent Transportation Systems (ITSC)*, pp. 3383-3389, 2023, <https://doi.org/10.1109/ITSC57777.2023.10422523>.
- [53] J. Li, J. Wu, and Y. Shao, "FSNB-YOLOV8: Improvement of object detection model for surface defects inspection in online industrial systems," *Appl. Sci. (Basel)*, vol. 14, no. 17, p. 7913, 2024, <https://doi.org/10.3390/app14177913>.

BIOGRAPHY OF AUTHORS

Erwin Sitompul, is an Associate Professor at the Study Program of Electrical Engineering, Faculty of Engineering, President University, Indonesia. He graduated from the Department of Physics Engineering, Bandung Institute of Technology, Indonesia, in 1998. Two years later he received the Master's degree in Electrical Engineering at the University of Kaiserslautern, Germany. In 2005 he obtained the doctorate in Automatic Control at the same university. His research interests include AI, neural networks, fuzzy logic, and robotics. He can be contacted at email: sitompul@president.ac.id.



Muhammad Teguh Ilham Yaqin, finished his Bachelor of Engineering in Electrical Engineering. Currently, he is an Engineer in PT. Global Adimitra Nusaabadi. He is certified in the field of Construction, Installation, and Maintenance of Low Voltage Power Distribution, SCADA, and Telecommunications at level 5. His main activity is related to Industrial Automation, SCADA, commissioning control panel protection for substations, power plants, and data centers. His email address is: mtilham24@gmail.com.



Hendra Jaya Tarigan, is an Assistant Professor of Electrical Engineering at Mississippi College (MC), USA. He earned a B.S. in Engineering Physics degree in 1988 and MS in Physics degree in 1992, both at the University of Nevada, Reno (UNR), USA. Further, he earned an M.S. in Applied Physics degree in 2012, M.S. in Electrical Engineering degree in 2013 and Ph.D. in Electrical Engineering degree in 2016, all three at Texas Tech University (TTU), USA. His research interests are nanophotonics and sensors. He can be contacted at email: htarigan@mc.edu.



George Michael Tampubolon, is a researcher and a Master's candidate in Mechanical Engineering at Pusan National University, South Korea. Since 2022, he has been a member of the Computer Aided Process Design Lab, where he engages in collaborative research between industries, academia, and the private sector. He earned his Bachelor's degree in Electrical Engineering from Institut Teknologi Nasional Bandung. His current research focuses on optimizing gerotor design using a Conditional Generative Adversarial Network (CGAN) to enhance hydraulic performance by generating smarter tooth profiles. His research interests include AI applications in mechanical design, deep learning, image processing, and machine learning-based optimization analysis. He also has experience in numerical simulations and engineering software, such as ANSYS Workbench, Inventor, and AutoCAD. His email address is: georgetampubolon@pusan.ac.kr.



Faisal Samsuri, completed his study in Electrical Engineering simultaneously with his various functions in various companies such as maintenance engineer, research assistant, service engineer, and firmware engineer. Currently, he is pursuing a Master's degree in Automation and Control at the Graduate Institute of Automation and Control, College of Engineering, National Taiwan University of Science and Technology. His focus research is in optical metrology, related to the measurement and control systems for critical dimension in the semiconductor manufacturing. His email address is: m11212803@mail.ntust.edu.tw.



Mia Galina, graduated from Brawijaya University with a Bachelor's degree in Electrical Engineering in 2001 and a Master's degree from the Universitas Indonesia in 2015. She is a lecturer in the Study Program of Electrical Engineering at President University and is pursuing a Doctorate in Electrical Engineering at Universitas Indonesia. Prior to joining President University, she worked for 15 years for a telecommunications company and as a consultant. Her research interests are IoT, sensors, and mobile wireless communications. She can be contacted at email: miagalina@president.ac.id.